Electronic Supplementary Information

Enantiopure natural deep eutectic solvents for metal-organic framework chiral induction

Renata A. Maia,[a] Audrey Fluck,[a] Catalin Maxim,[b] Benoît Louis,[c,*] Stéphane A. Baudron [a,*]

a. Université de Strasbourg, CNRS, CMC UMR 7140, 4 rue Blaise Pascal, F-67000 Strasbourg, France. E-mail : sbaudron@unistra.fr

b. University of Bucharest, Faculty of Chemistry, Inorganic Chemistry Laboratory, Str. Dumbrava Rosie 23, 020464 Bucharest, Romania

c. Université de Strasbourg, CNRS, ICPEES UMR 7515, 25 rue Becquerel, F-67087 Strasbourg, France. E-mail : blouis@unistra.fr

Experimental Section

Materials

The commercially available reagents choline chloride (99% purity, Acros), *L*-proline (99% purity, Sigma-Aldrich), *D*-proline (99% purity, ABCR), *DL*-proline (98% purity, BLDpharm), *L*-menthol (≥ 99% purity, Sigma-Aldrich), *D*-menthol (≥ 99% purity, TCI Chemicals), *DL*-menthol (99% purity, Acros), thymol (≥ 99% purity, Sigma-Aldrich), $TbCl_3.6H_2O$ (99.9% purity, Strem Chemicals or Sigma-Aldrich), 1,3,5-benzenetribenzoic acid (prepared as described[1] or purchased from BLD pharm, 95% purity) were used as received.

Synthesis

General preparation of the deep eutectic solvents: in a round bottom flask, equipped with a stirring bar, it was added, in the respective molar ratio (see Table 1), the DES components. The flask was placed in a pre-heated oil bath at 100 °C and the mixture was stirred until it became a clear liquid solution. Due to their viscosity, the DESs were kept at 100 °C to facilitate the addition of these solvents into the reaction vessel by syringe. The DESs were freshly prepared right before each reaction.

Synthesis of MIL-103: In a 48 mL Chemglass vessel, $TbCl_3.6H_2O$ (1 equiv., 1.71 mmol, 0.64 g), 1,3,5-benzenetribenzoic acid (1 equiv., 1.71 mmol, 0.75 g) and NaOH 2 M solution (1.8 equiv. 3.0 mmol, 1.5 mL) were added. With the aid of a syringe, 12.5 mL of the appropriate deep eutectic solvent was added into the reaction vessel. Right after, the vessel was sonicated at 40 °C for 1 h to homogenize the reaction mixture before the reaction. Then, the vessel was placed in a pre-heated oil bath at 120 °C for 3 days. At the end of the reaction, the vessel was cooled down to room temperature. The workup of the reaction consists in washing the solid product in a Büchner funnel according to the following steps. First, distilled water (15 mL) was poured into the reaction vessel and the slurry was mixed by a spatula. After, it was filtered off and washed with more water (30 mL). Then, the brownish solid was washed with DMF until the filtrate became clear and the solid became white/off-white. The DMF was then washed off from the solid with water (30 mL), followed by ethanol (30 mL). The remaining solid product was immersed in ethanol (100 mL) for a week, and every two days the ethanol was replaced for a fresh one. Finally, the solid was again filtered off and dried in an oven at 80 °C overnight. The remaining product was analyzed by PXRD, TGA, elemental analysis, infra-red spectroscopy, and N_2 adsorption-desorption isotherms at 77 K.

Table ESI1

MOF(Tb)	DES	Mass (g)	T_d (°C)	S_{BET} (m^2/g)	Elemental analysis (%)	CD (mdeg)
***D*-pro-MIL-103**	(1:7) *D*- proline:thymol	1.478[a]	588	630	**Found:** N 0.19, C 53.25, H 2.64 **Calcd:** N 0.19, C 53.33, H 2.82 for $Tb(BTB)(H_2O)_{0.75}(D\text{-}pro)_{0.08}$	- 6.4
***L*-pro-MIL-103**	(1:7) *L*-proline:thymol	1.346[a]	588	592	**Found:** N 0, C 52.05, H 2.58 **Calcd:** N 0, C 52.04, H 2.94 for $Tb(BTB)(H_2O)_{1.60}$	+ 5.4
***DL*-pro-MIL-103**	(1:7) *DL*-proline:thymol	0.736	580	787	**Found:** N 0.30, C 51.35, H 2.66 **Calcd:** N 0.36, C 51.47, H 3.18 for $Tb(BTB)(H_2O)_{2.0}(DL\text{-}pro)_{0.17}$	0
***D*-men-MIL-103**	(1:1) *D*-menthol/thymol	0.645	581	633	[b]	+ 2.8
***L*-men-MIL-103**	(1:1) *L*-menthol/thymol	0.662	581	758	[b]	- 2.9
***DL*-men-MIL-103**	(1:1) *DL*-menthol/thymol	0.589	580	589	[b]	0
water:cyclohexanol MIL-103	water:cyclohexanol (1:1)	0.656	578	1087	**Found:** N 0, C 53.36, H 2.45 **Calcd:** N 0, C 53.35, H 2.74 for $Tb(BTB)(H_2O)_{0.75}$	0

[a] The scale for this reaction has been doubled compared with the general protocol.

[b] No stable nor repeatable CHN analysis.

X-ray diffraction

PXRD patterns were recorded on a Bruker D8 Advance diffractometer with LynxEye detector, Cu K_α wavelength, in a 2θ interval of 4° – 40°, step size of 0.007° and time/step of 0.35 s.

Thermogravimetric analysis

The thermal stability of the samples was accessed in a PerkinElmer Thermogravimetric Analyzer TGA 4000 under N_2 flow of 20 mL/min, and a heating rate of 5 °C/min, up to 800 °C.

Gas sorption

The textural properties of the samples were obtained by N_2 adsorption-desorption isotherms at 77 K, in a Micromeritics ASAP 2020 Surface Area and Porosity Analyzer. The Brunauer-Emmett-Teller (BET) method was used for obtaining the total specific surface area (S_{BET}) and the pore size (model: NLDFT for cylinder pores). The samples were activated, prior to the N_2 adsorption-desorption analysis, by heating the sample under vacuum at 150 °C for 15 h. The MicroActive Software version 4.00 was used to analyze the data.

Elemental analysis

Elemental analyses (CHN) were performed at the *Service Commun d'Analyses* of the University of Strasbourg, in duplicate, employing a ThermoFischer Flash 2000 equipment, where the reported values for the CHN were taken as the average of two measurements.

Fourier-transform infrared spectroscopy

The infrared spectra were obtained in a FTIR-UATR PerkinElmer Spectrum Two, in the wavenumber interval of 4.000 cm^{-1} – 400 cm^{-1}.

Scanning electron microscopy

SEM images were obtained with a Zeiss GeminiSEM 500 microscope with a FEG Schottky source and an Everhart–Thornley detector.

Circular dichroism

Diffuse-reflectance circular dichroism (DRCD) spectra (room temperature) of crystalline samples were performed on a JASCO J-1500 spectrophotometer equipped with an integrating sphere attachment (DRCD-575 accessory) in the 200-800 nm domain at a scan rate of 100 nm/min and accumulated twenty times.

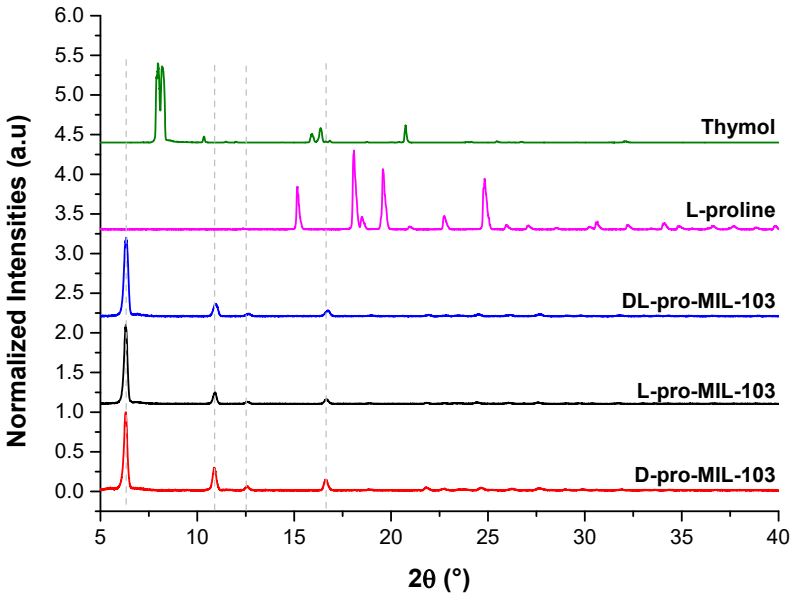

Fig. ESI1 – PXRD patterns of the DES components thymol and L-proline, and of the MIL-103(Tb) MOFs prepared in *D*-proline:thymol, *L*-proline:thymol, *DL*-proline:thymol.

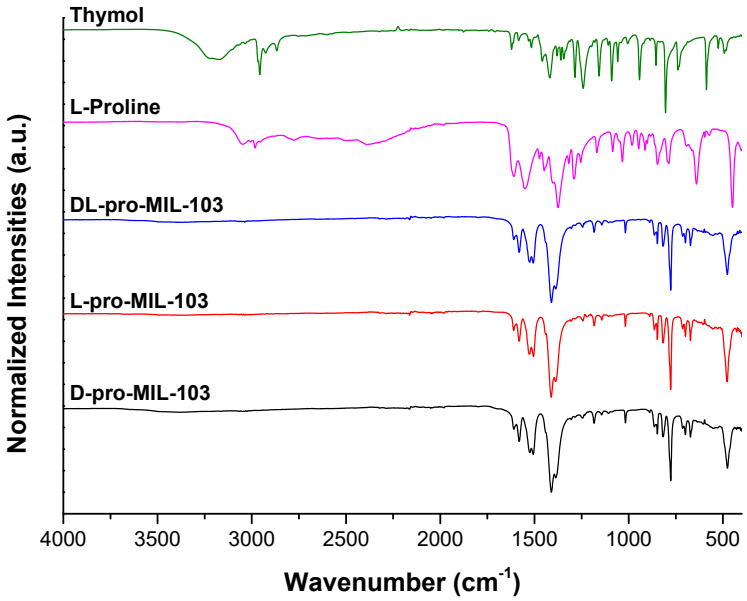

Fig. ESI2 – FT-IR spectra of the DES components thymol (green) and L-proline (pink), and of the MIL-103(Tb) prepared in *D*-proline:thymol (black), *L*-proline:thymol (red), *DL*-proline:thymol (blue).

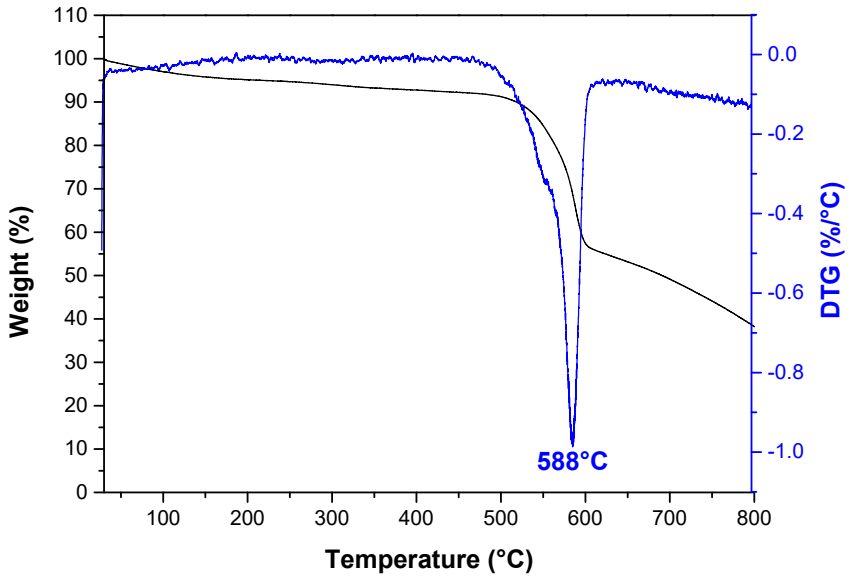

Fig. ESI3 – TGA plot of *D*-pro-MIL-103(Tb).

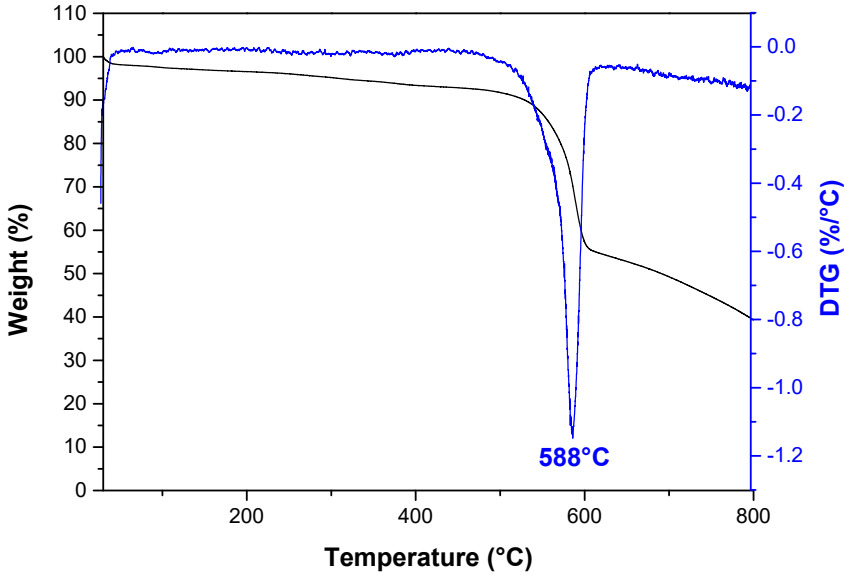

Fig. ESI4 – TGA plot of *L*-pro-MIL-103(Tb).

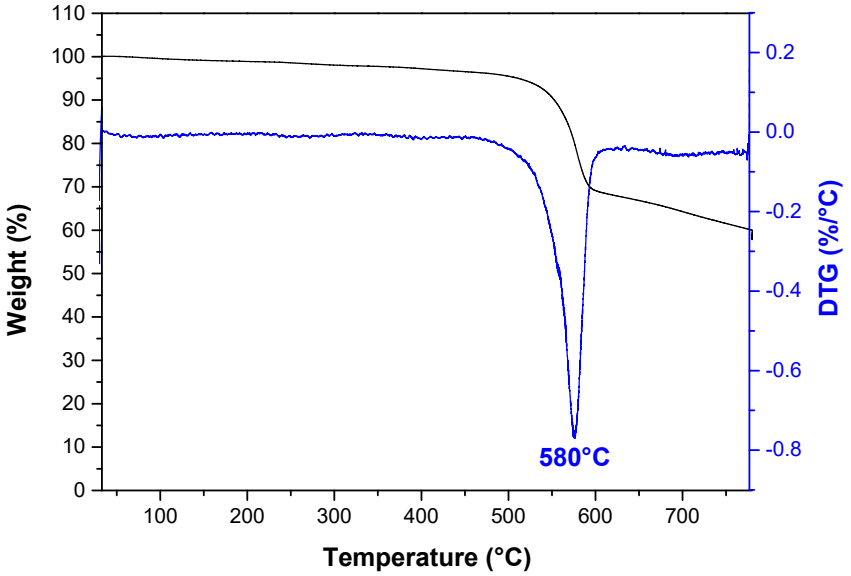

Fig. ESI5 – TGA plot of *DL*-pro-MIL-103(Tb).

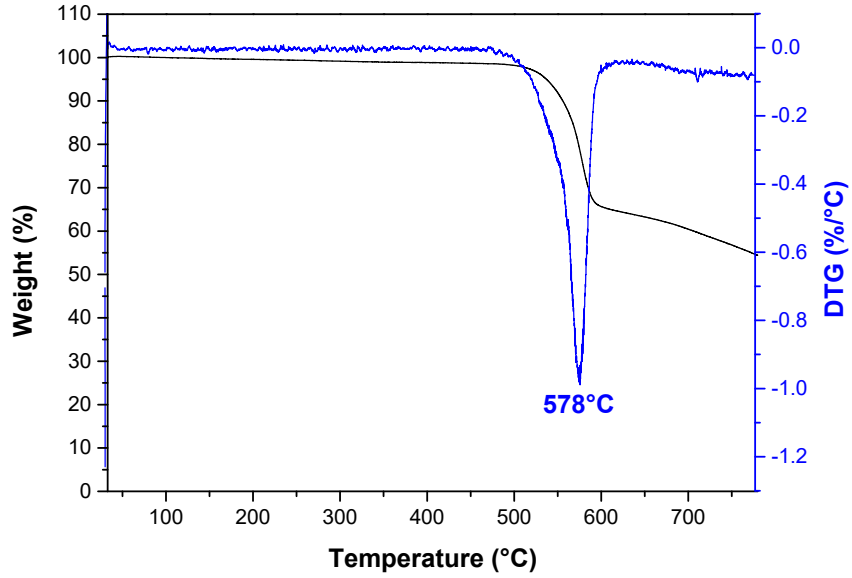

Fig. ESI6 – TGA plot of water:cyclohexanol MIL-103(Tb).

Table ESI2. Data presented in Fig. 4

MOF	CD (mdeg)
L-pro-MIL-103(Tb) before activation	+5.0 (at 317 nm)
D-pro-MIL-103(Tb) before activation	-7.7 (at 316 nm)
L-pro-MIL-103(Tb) after activation	+5.5 (at 318 nm)
D-pro-MIL-103(Tb) after activation	-6.4 (at 318 nm)

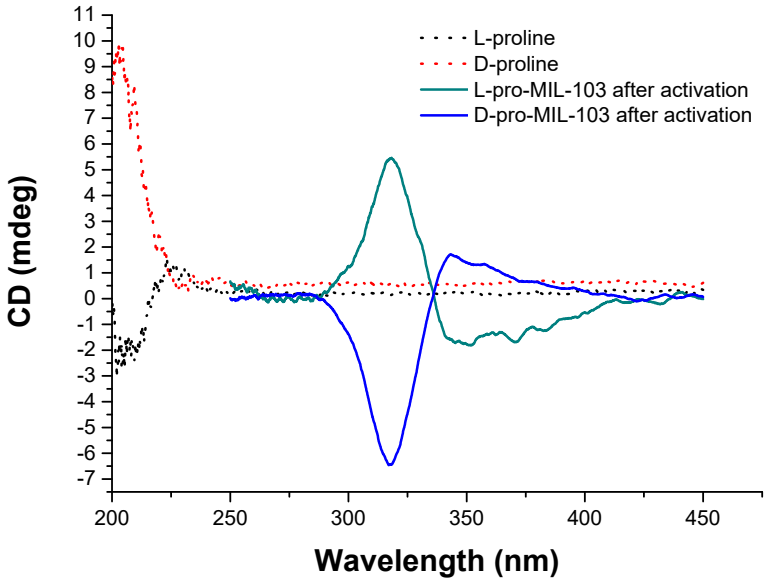

Fig. ESI7 – Circular dichroism spectra of the chiral MIL-103(Tb) MOFs prepared in different solvents: *D*-proline:thymol, and *L*-proline:thymol (after activation) and comparison with the DES components *D*- and *L*-proline.

Table ESI3. Extension of proline-based MOFs to other lanthanides (no sample was activated – the MOF was just filtered off and washed with DMF, water, and ethanol). Data presented in Fig. 5.

	CD (mdeg)
L-pro-MIL-103 (Tb)	+6.8 (at 323 nm)
D-pro-MIL-103 (Tb)	-5.9 (at 323 nm)
L-pro-MIL-103 (Eu)	+13.7 (at 317 nm)
D-pro-MIL-103 (Eu)	-17.3 (at 318 nm)
L-pro-MIL-103 (Nd)	+40.2 (at 317 nm), +6.0 (at 585 nm), +4.2 (741 nm)
D-pro-MIL-103 (Nd)	-44.5 (at 318 nm), -6.0 (at 580 nm), -4.1 (740 nm)

* For MIL-103(Tb), the batches are different from the MIL-103(Tb) ones listed in tableESI2.

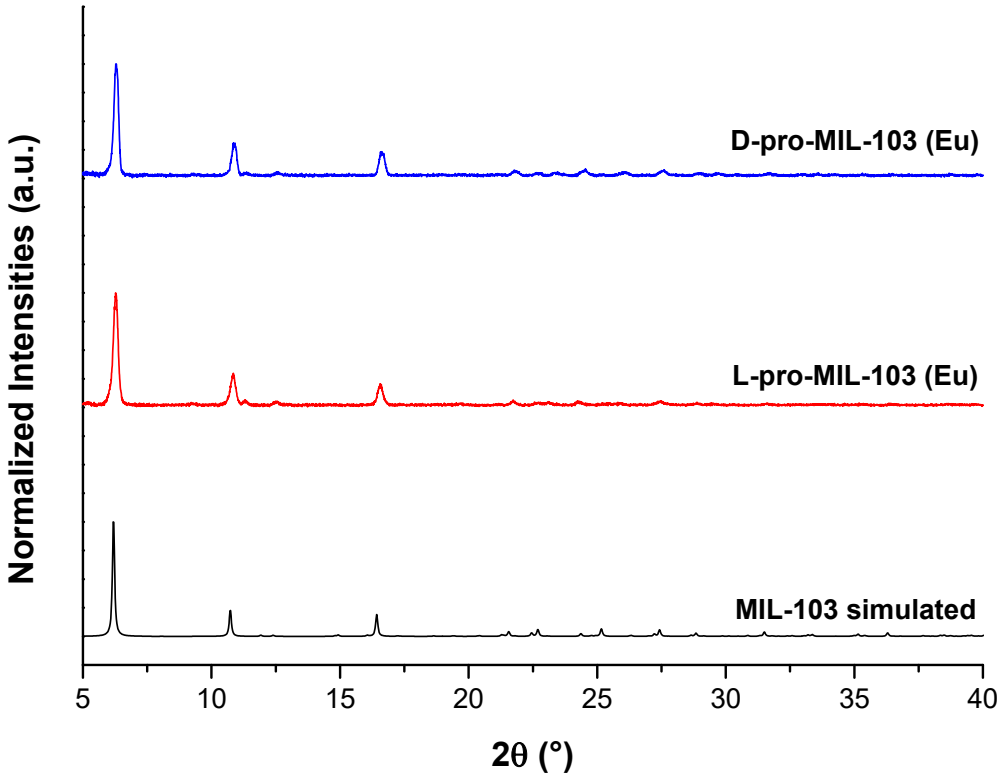

Fig. ESI8 – PXRD patterns of the MIL-103(Eu) MOFs prepared in *D*-proline:thymol and *L*-proline:thymol.

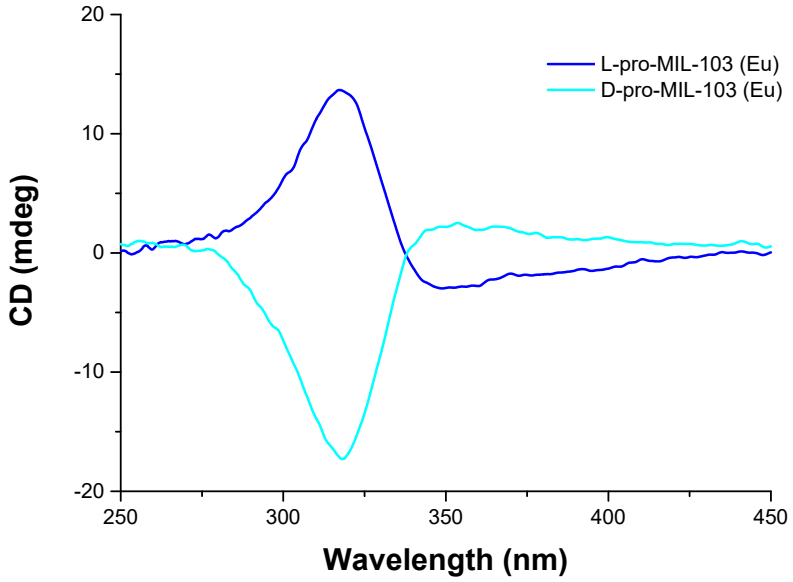

Fig. ESI9 – Circular dichroism spectra of the chiral MIL-103(Eu) MOFs prepared in different solvents: *D*-proline:thymol, and *L*-proline:thymol.

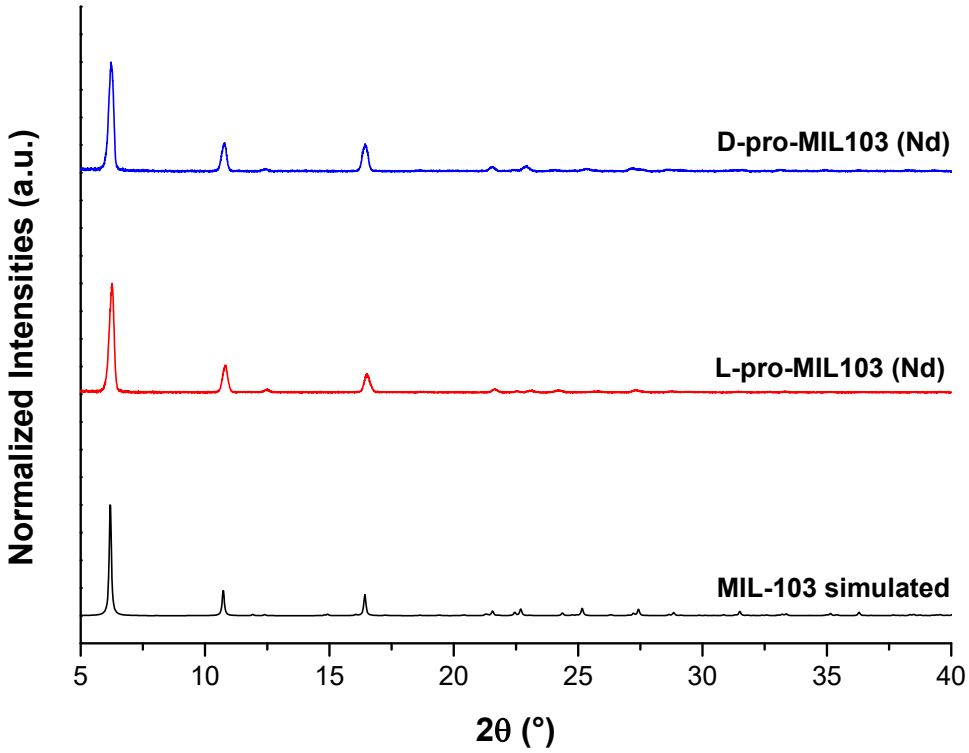

Fig. ESI10 – PXRD patterns of the MIL-103(ND) MOFs prepared in *D*-proline:thymol and *L*-proline:thymol.

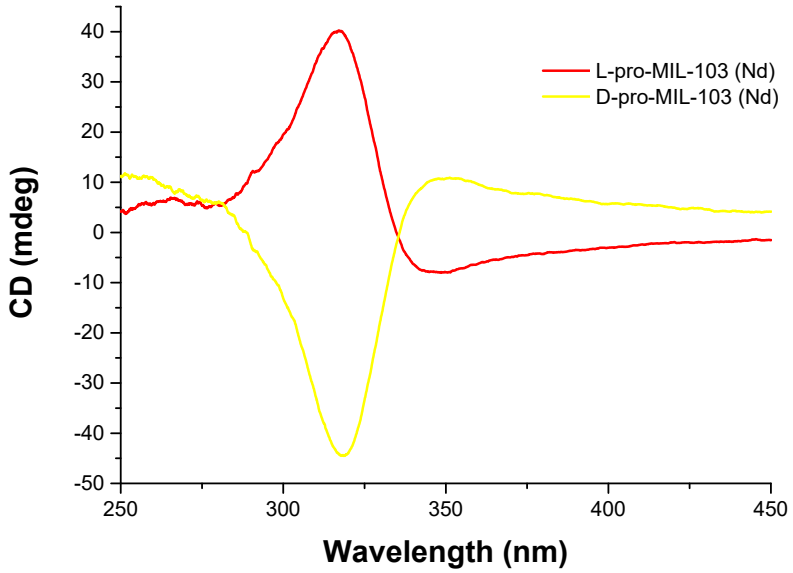

Fig. ESI11 – Circular dichroism spectra of the chiral MIL-103(Nd) MOFs prepared in different solvents: *D*-proline:thymol, and *L*-proline:thymol.

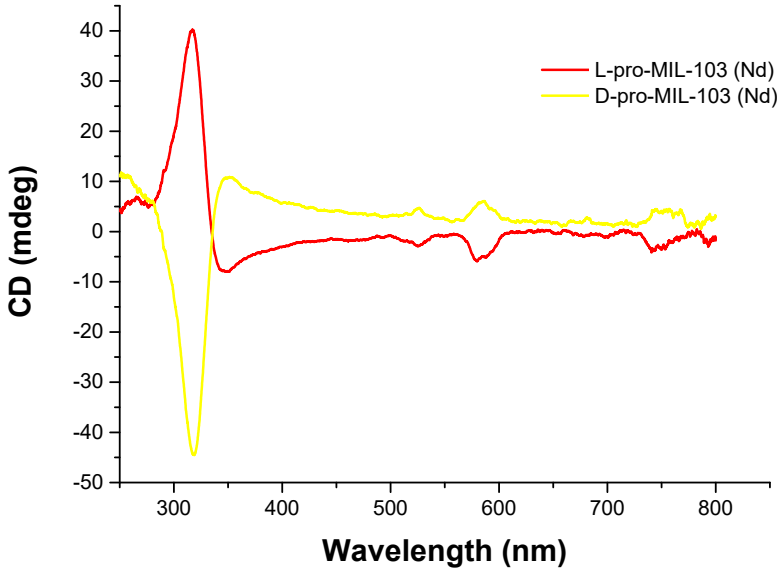

Fig. ESI12 – Circular dichroism spectra of the chiral MIL-103 MOFs (Nd) prepared in different solvents: *D*-proline:thymol, and *L*-proline:thymol.

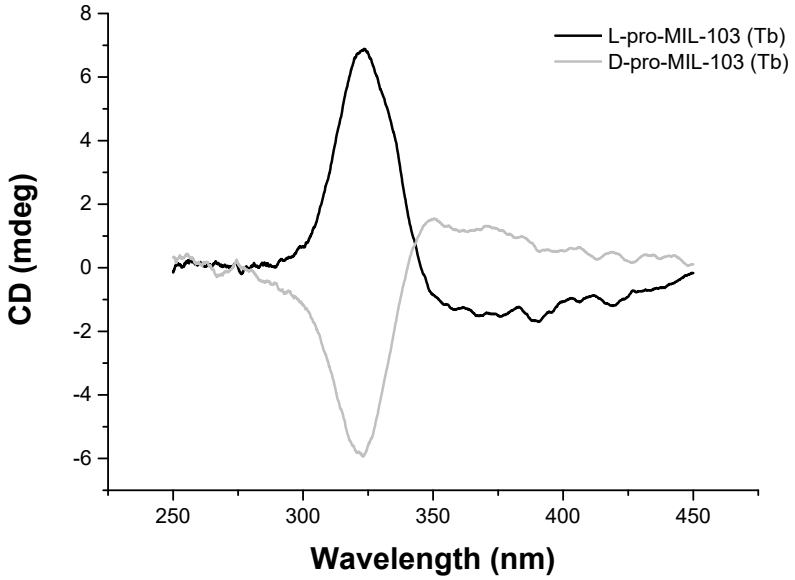

Fig. ESI13 – Circular dichroism spectra of the chiral MIL-103(Tb) MOFs prepared in different solvents: *D*-proline:thymol, and *L*-proline:thymol.

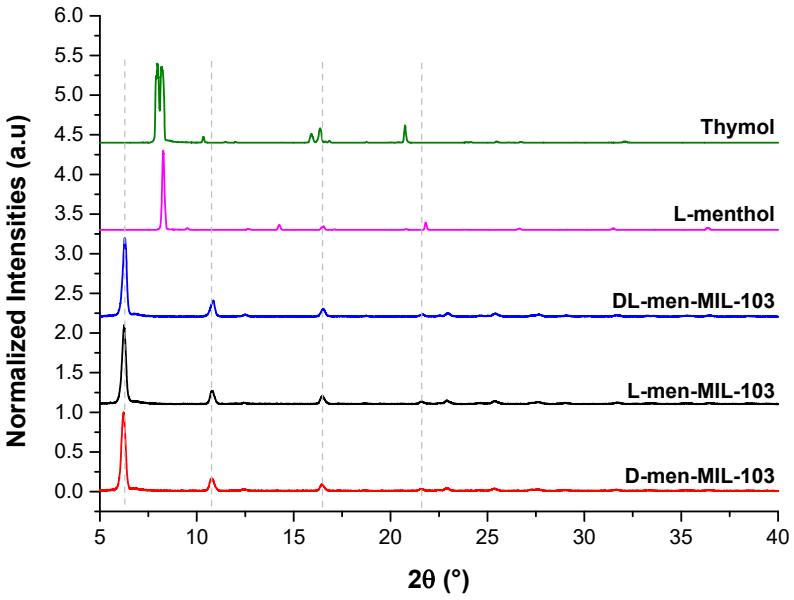

Fig. ESI14 - PXRD patterns of the DES components thymol and *L*-menthol, and of the MIL-103(Tb) MOFs prepared in *D*-menthol:thymol, *L*-menthol:thymol, *DL*-menthol:thymol.

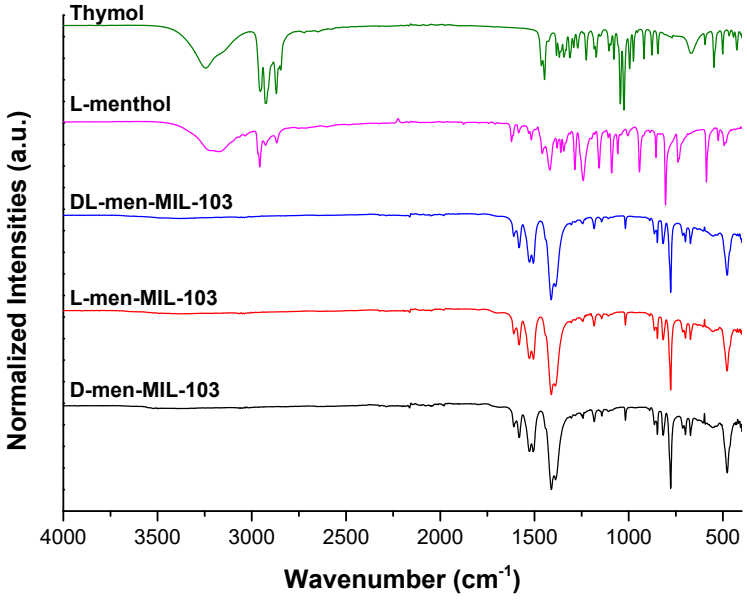

Fig. ESI15 – FT-IR spectra of the DES components thymol (green) and *L*-menthol (pink), and of the MIL-103(Tb) MOFs prepared in *D*-menthol:thymol (black), *L*-menthol:thymol (red), *DL*-menthol:thymol (blue).

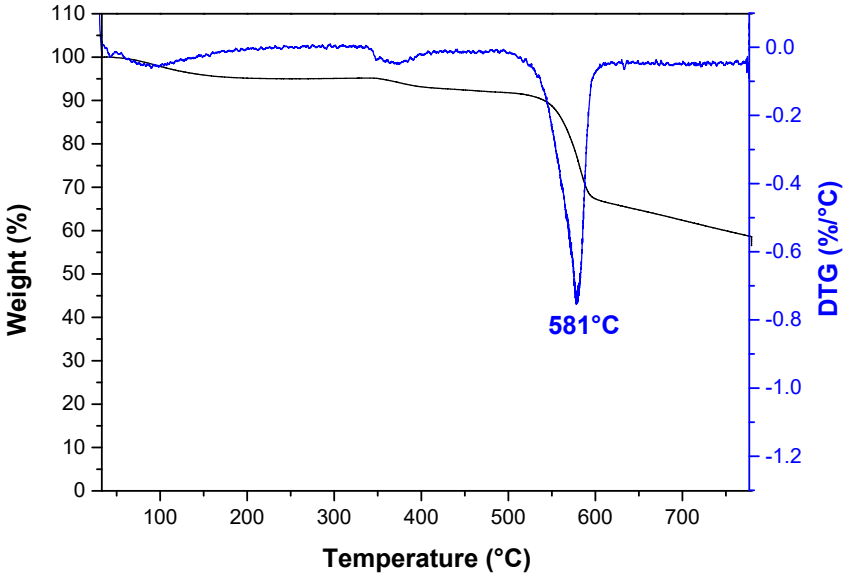

Fig. ESI16 – TGA plot of *D*-men-MIL-103(Tb).

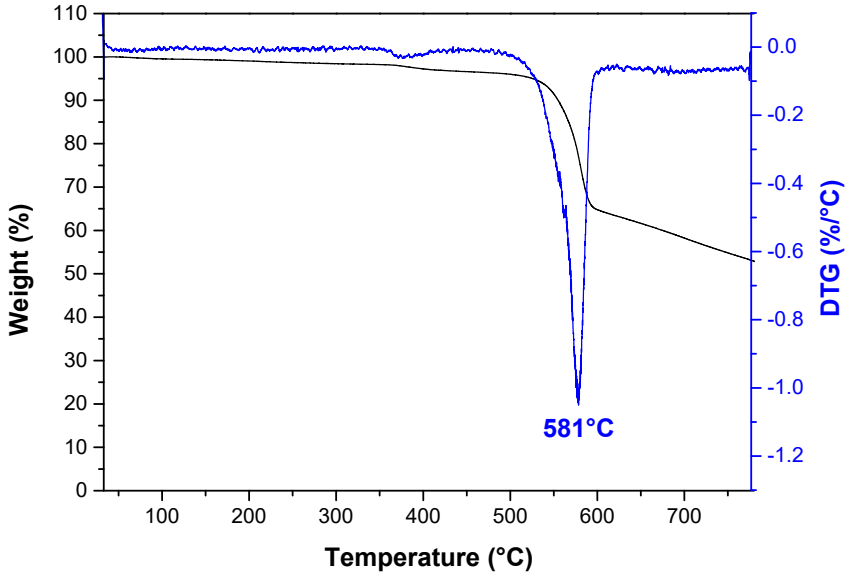

Fig. ESI17 – TGA plot of *L*-men-MIL-103(Tb).

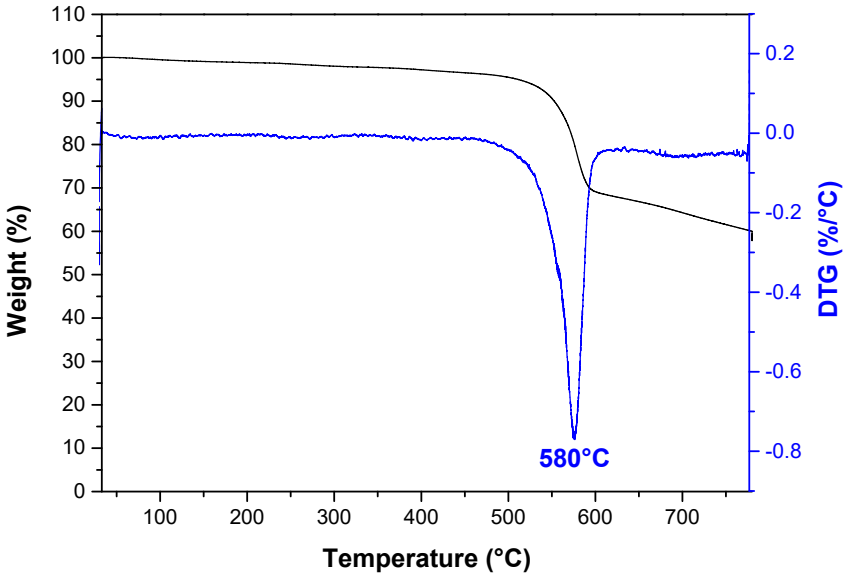

Fig. ESI18 – TGA plot of *DL*-men-MIL-103(Tb).

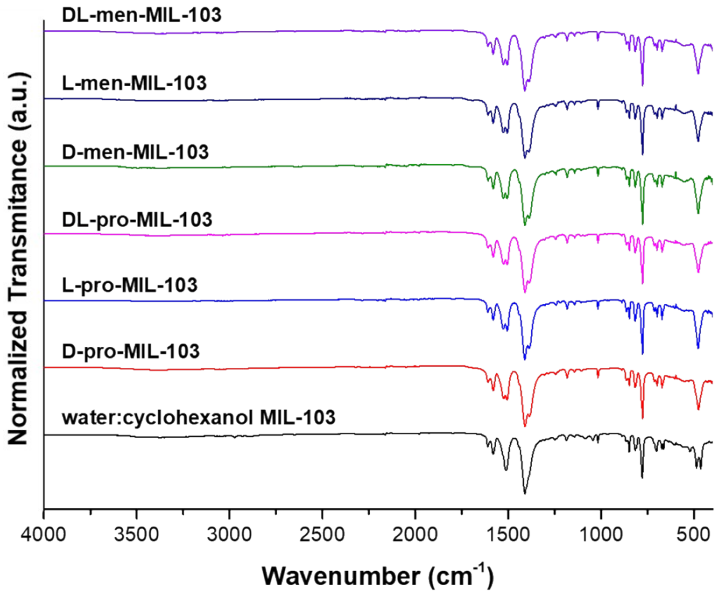

Fig. ESI19. FT-IR spectra of the MIL-103(Tb) MOFs prepared in different solvents: water:cyclohexanol, *D*-proline:thymol, *L*-proline:thymol, *DL*-proline:thymol, *D*-menthol:thymol, *L*-menthol:thymol, *DL*-menthol:thymol.

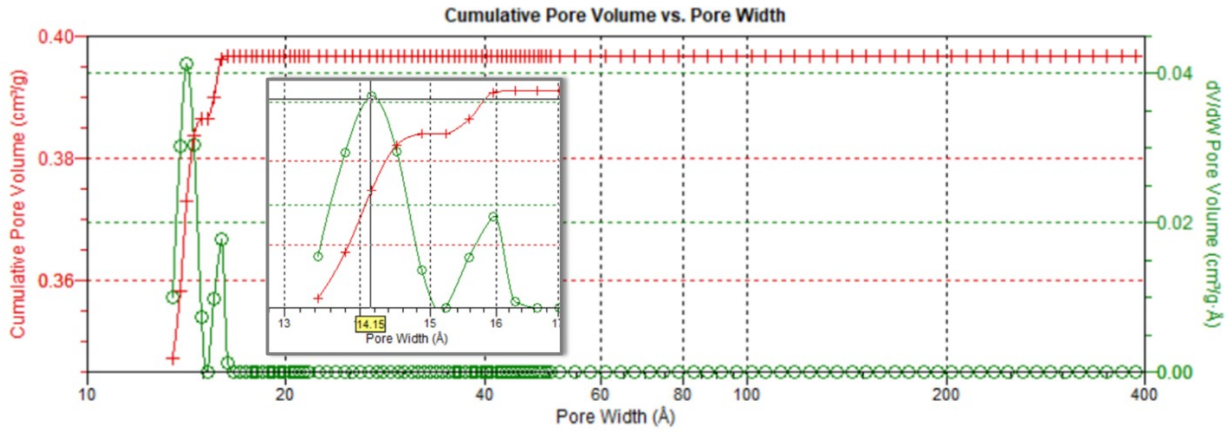

Fig. ESI20. Pore size distribution for the water:cyclohexanol MIL-103 MOF.

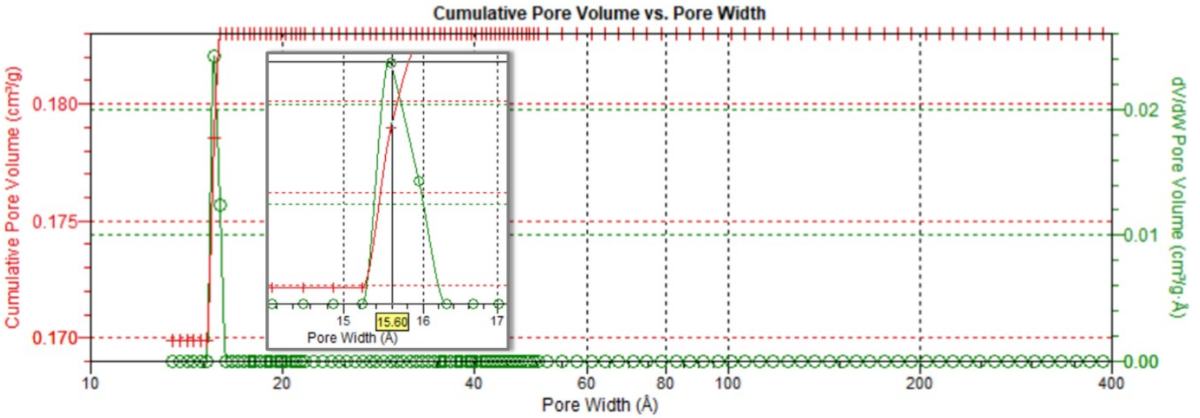

Fig. ESI21. Pore size distribution for the *L*-pro-MIL-103 MOF.

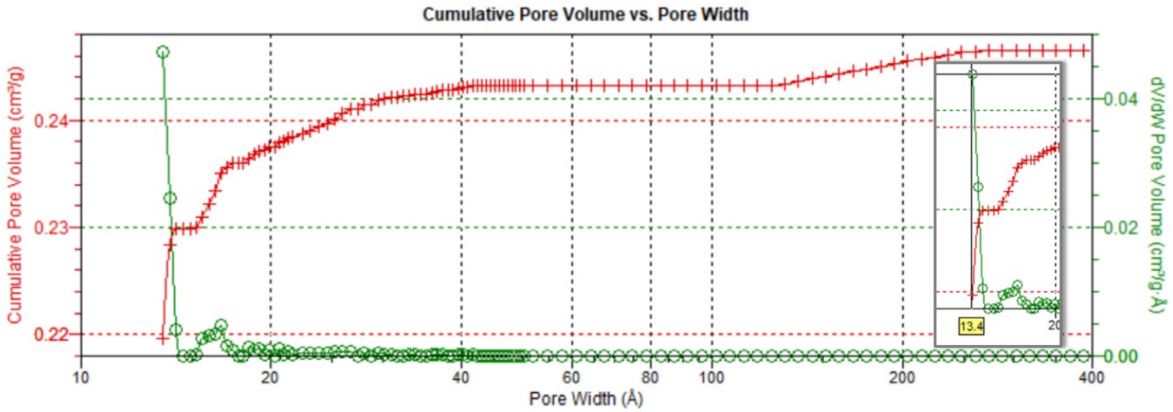

Fig. ESI22. Pore size distribution for the *D*-pro-MIL-103 MOF.

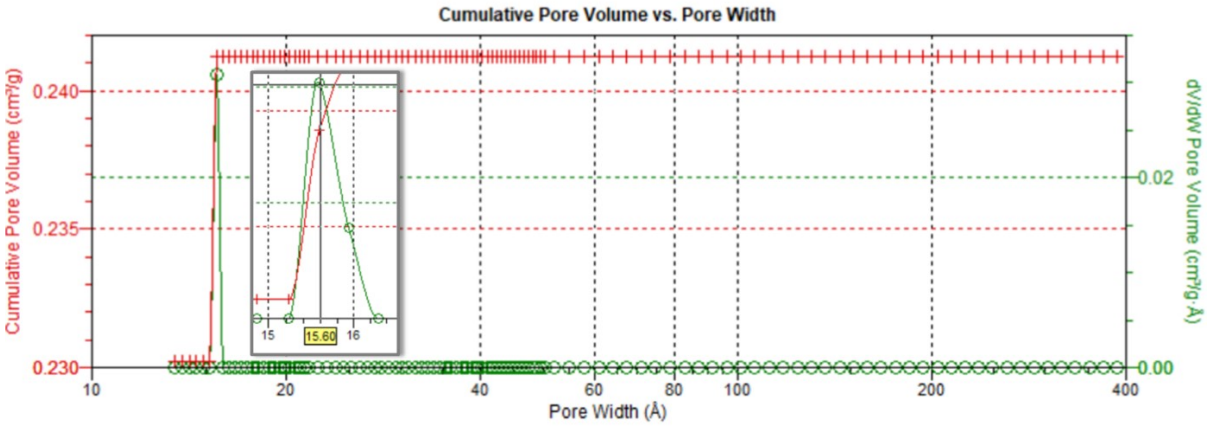

Fig. ESI23.. Pore size distribution for the *DL*-pro-MIL-103 MOF.

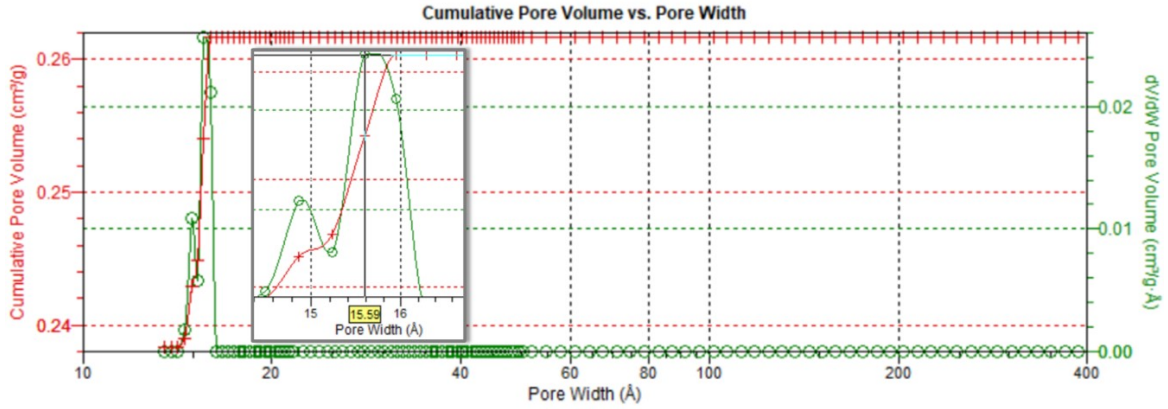

Fig. ESI24. Pore size distribution for the *L*-men-MIL-103 MOF.

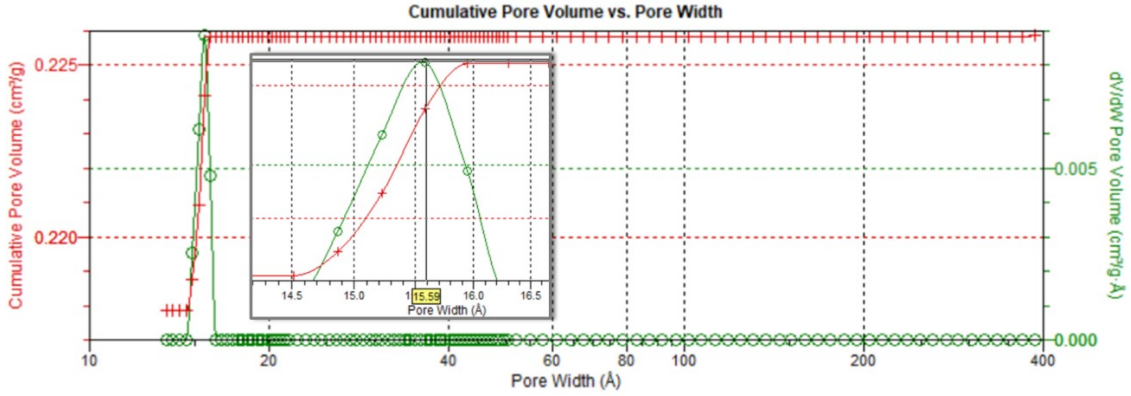

Fig. ESI25. Pore size distribution for the *D*-men-MIL-103 MOF.

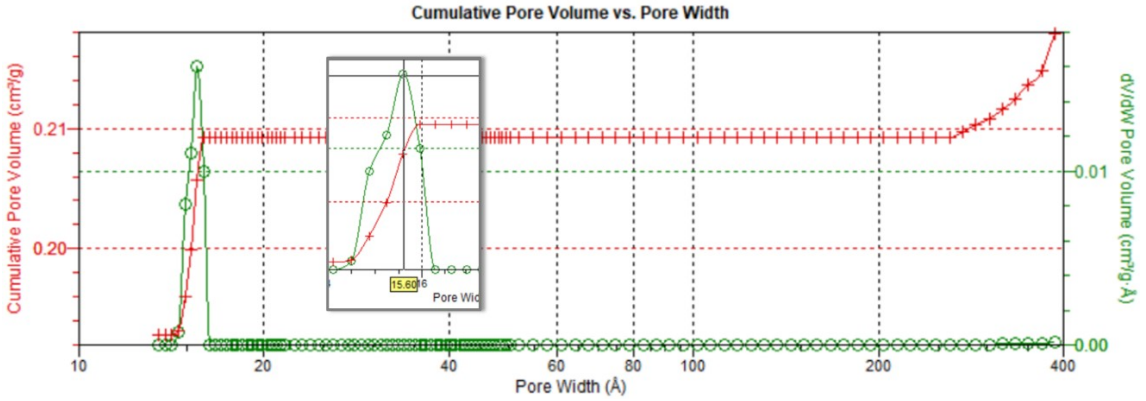

Fig. ESI26. Pore size distribution for the DL-men-MIL-103 MOF.

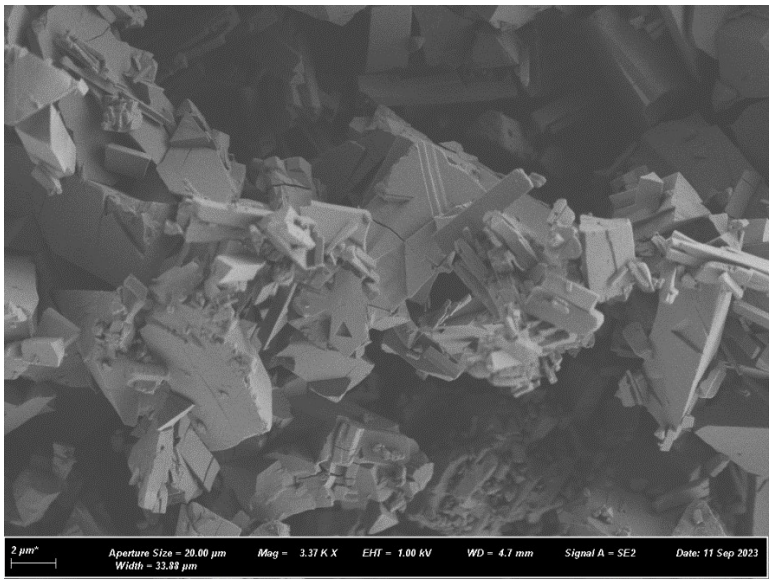

Fig. ESI27. SEM micrograph of the water:cyclohexanol MIL-103(Tb) MOF.

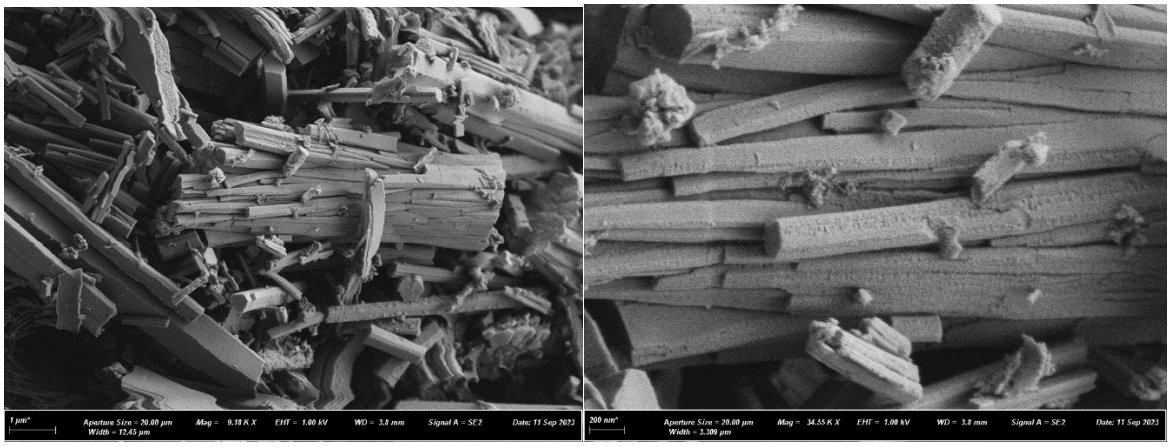

Fig. ESI28. SEM micrographs of the *L*-pro MIL-103(Tb) MOF.

Fig. ESI29. SEM micrograph of the *D*-pro MIL-103(Tb) MOF.

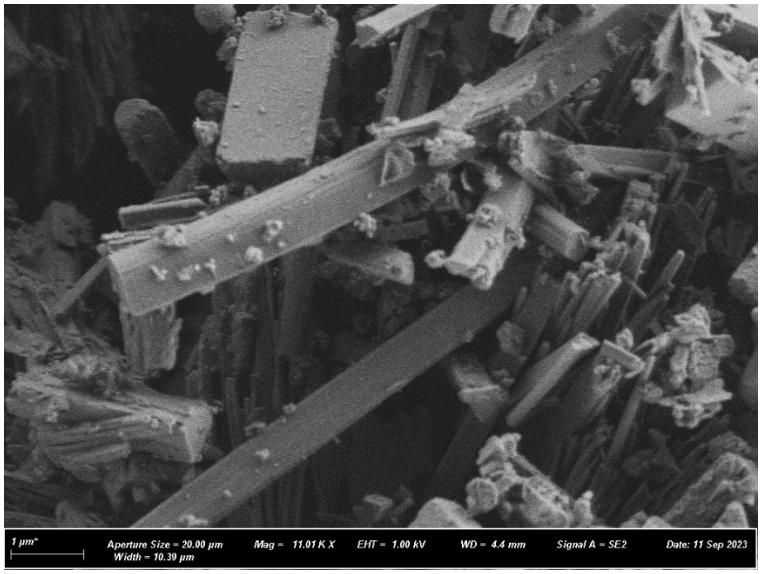

Fig. ESI30. SEM micrograph of the *DL*-pro MIL-103(Tb) MOF.

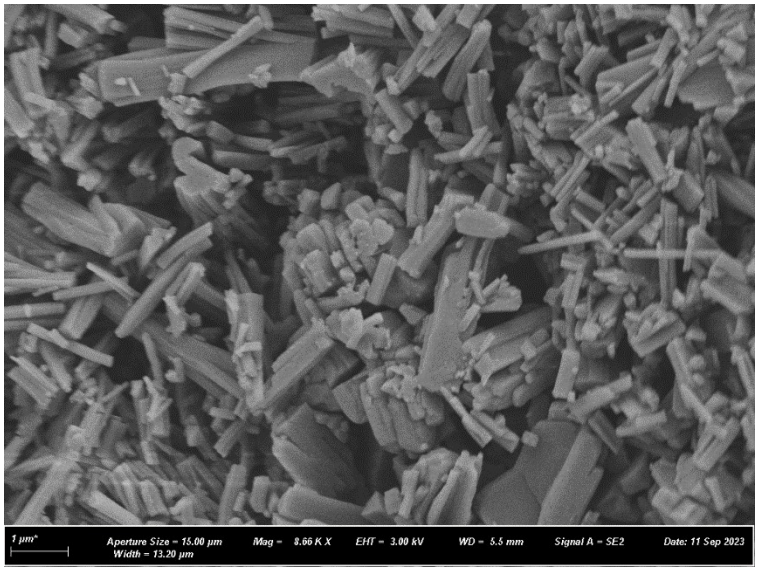

Fig. ESI31. SEM micrograph of the *L*-men MIL-103(Tb) MOF.

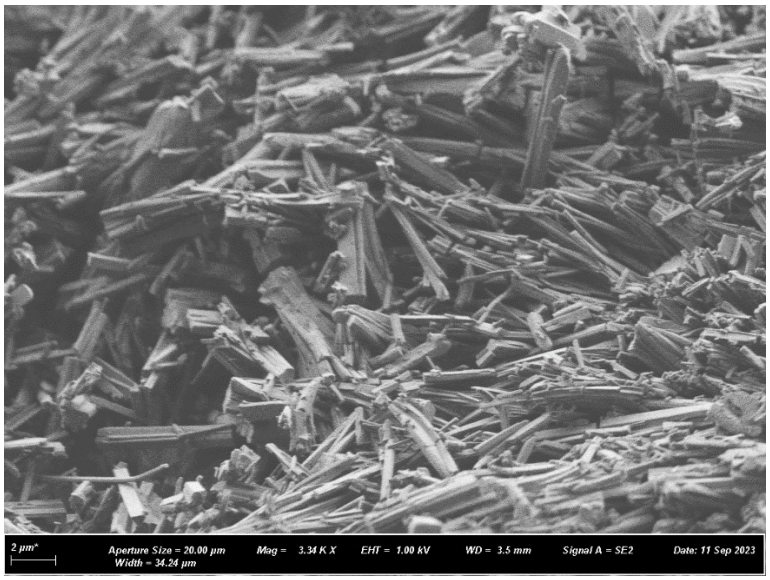

Fig. ESI32. SEM micrograph of the *D*-men MIL-103(Tb) MOF.

Fig. ESI33. SEM micrograph of the *DL*-men MIL-103(Tb) MOF.

Reference

1. D. J. Tranchemontagne, L. Dudek and O. M. Yaghi, *Inorg. Synth.*, 2010, **35**, 102